A chamber study of alkyl nitrate production formed by terpene ozonolysis in the presence of NO and alkanes

CrossMark

Stephen R. Jackson, Joel C. Harrison, Jason E. Ham, J.R. Wells[*]

Exposure Assessment Branch, Health Effects Laboratory Division, National Institute for Occupational Safety and Health, 1095 Willowdale Road, Morgantown, WV 26505, United States

H I G H L I G H T S

- Description of ethyl acetate as an impinger medium for collection of gas-phase organic nitrates.
- Quantified alkyl nitrate formation initiated by terpene ozonolysis for a range of ozone and NO concentrations.
- Ozone and NO concentrations near 100 ppb resulted in the highest organic nitrate yield observed, roughly 5 ppb.

A R T I C L E   I N F O

A B S T R A C T

Organic nitrates are relatively long-lived species and have been shown to have a potential impact on atmospheric chemistry on local, regional, and even global scales. However, the significance of these compounds in the indoor environment remains to be seen. This work describes an impinger-based sampling and analysis technique for organic nitrate species, focusing on formation via terpene ozonolysis in the presence of nitric oxide (NO). Experiments were conducted in a Teflon film environmental chamber to measure the formation of alkyl nitrates produced from α-pinene ozonolysis in the presence of NO and alkanes using gas chromatography with an electron capture detector. For the different concentrations of NO and O_3 analyzed, the concentration ratio of $[O_3]/[NO]$ around 1 was found to produce the highest organic nitrate concentration, with $[O_3] = 100$ ppb & $[NO] = 105$ ppb resulting in the most organic nitrate formation, roughly 5 ppb. The experiments on α-pinene ozonolysis in the presence of NO suggest that organic nitrates have the potential to form in indoor air between infiltrated ozone/NO and terpenes from household and consumer products.

Published by Elsevier Ltd.

1. Introduction

The use of cleaning agents and air fresheners in buildings exposes occupants, especially cleaning personnel, to a wide variety of airborne chemicals (Bello et al., 2009; Gerster et al., 2014; Wolkoff et al., 1998). While many of these chemicals are deemed safe, they can react with other air contaminants to yield potentially harmful secondary products (Nazaroff and Weschler, 2004). For example, terpenes, such as α-pinene, limonene, and terpinolene, can react rapidly with ozone in indoor air producing many secondary pollutants including formaldehyde (Nazaroff and Weschler, 2004). Furthermore, it has previously been shown that ozone-terpene reactions produce the hydroxyl radical, which reacts rapidly with
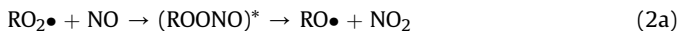
organic compounds, leading to the formation of other potentially toxic air pollutants (Nazaroff and Weschler, 2004; Wolkoff et al., 1998).

In the presence of NO_x ($NO + NO_2$), one class of compounds that can be generated from hydroxyl radical reactions is organic nitrates (Arey et al., 1990). Organic nitrates have been observed in the atmosphere for decades and are thought to make up a significant fraction of the total atmospheric nitrogen oxides (Day et al., 2009; Rollins et al., 2010). Hydrocarbon oxidation in the atmosphere is initiated by free radicals, particularly hydroxyl radicals (•OH), which react by hydrogen abstraction or addition (in the case of unsaturated compounds) (Monks, 2005) to form alkyl radicals (R•) which further react with oxygen to generate peroxyl radicals (RO_2•), (Reaction (1)). Peroxyl radicals can subsequently react with nitric oxide (NO) to form an alkoxy radical and NO_2 (Reaction (2a)) or alkyl nitrates (Reaction (2b)). (Atkinson and Arey, 2003; Atkinson

et al., 1983; Yeh and Ziemann, 2014). Furthermore, alkyl nitrates may form through alkoxyl radical reaction with NO_2 (Reaction (3)).

$$R\bullet + O_2 + M \rightarrow RO_2\bullet + M \tag{1}$$

$$RO_2\bullet + NO \rightarrow (ROONO)^* \rightarrow RO\bullet + NO_2 \tag{2a}$$

$$RO_2\bullet + NO \rightarrow (ROONO)^* \rightarrow RONO_2 \text{ (alkyl nitrate)} \tag{2b}$$

$$RO\bullet + NO_2 + M \rightarrow RONO_2 \tag{3}$$

While organic nitrates have been shown to contribute significantly to the sum total nitrogen in the atmosphere, their presence indoors has yet to be determined. Organic nitrates have the opportunity to form indoors through the same mechanisms as those formed in the troposphere. Alkenes known to have significant indoor concentrations (α-pinene, ᴅ-limonene, and α-terpinene) react with O_3 at rates faster than typical air exchange rates, producing meaningful yields of OH radicals (Forester and Wells, 2011; Weschler and Shields, 1996). Motivated by knowledge gaps in exposure assessment, significant progress has been made in detection and characterization methods for many of the oxygenated species resulting from O_3/alkene reactions; however, characterization of organic nitrate formation has been marginal.

Given the potential importance of the NO oxidation channel and the current lack of experimental data on organic nitrate formation, this study explored α-pinene ozonolysis in the presence of NO concentrations that have been measured indoors (Weschler and Shields, 1997; Weschler et al., 1994). An impinger-based technique was utilized to collect organic nitrate products formed in chamber reactions, and the products were analyzed using gas chromatography with an electron capture detector (GC-ECD). The levels of ozone and NO in the chamber were varied to identify the conditions most suitable for organic nitrate formation.

2. Experimental methods

2.1. Materials

Isopropyl nitrate (≥98.0%), isobutyl nitrate (96%), 2-ethylhexyl nitrate (97%), (+)-α-pinene (≥99%), cyclohexane (HPLC grade, ≥99.9%), toluene (HPLC grade, ≥99.9%), hexane (≥99%), bromocyclohexane (98%), silver nitrate (≥99.0%), and acetonitrile (biotech grade, ≥99.93%) were purchased from Sigma-Aldrich (St. Louis, MO). Methanol (HPLC grade ≥99%), ethyl acetate (99.9%), and methylene chloride (99.9%) were purchased from Fisher Scientific. Deionized water (DI H_2O) was distilled, deionized to a resistivity of 18 MΩ cm, and filtered using a Milli-Q® filter system (Billerica, MA). Helium and N_2 (UHP grades) were supplied by Butler Gas (McKees Rocks, PA) and used as received.

Experiments were performed at 297 ± 3 K and 1 atm in a collapsible 80 L reaction chamber that has been described previously (Ham et al., 2015, 2016; Jackson et al., 2017). Briefly, the collapsible reaction chamber was constructed from 5-mil fluorinated ethylene propylene copolymer (FEP) Teflon film (Welch Fluorocarbon Inc., Dover, NH) and sealed using a W-600T double foot sealer (Sealer Sales, Northridge, CA). Compressed air was provided from the National Institute for Occupational Safety and Health (NIOSH) facility and was passed through anhydrous $CaSO_4$ (Drierite, Xenia, OH) to remove moisture. Compressed air flowed through a mass flow controller (MKS, Andover, MA) and into a humidifying chamber where it was mixed with dry air to the predetermined relative humidity (RH) of 50%. The 80 L reaction chamber was equipped with a heated syringe injection port constructed of a 6.4-mm Swagelok (Solon, OH) tee fitting with a 10 mm

septum (Restek, Bellefonte, PA) which allowed for the introduction of liquid reactants into the chamber with the flowing air stream. Ozone was produced by photolyzing air with a mercury pen lamp (Jelight, Irvine, CA) in a separate Teflon chamber. Aliquots of this O_3/air mixture were added to the 80 L Teflon reaction chamber using a gas-tight syringe. O_3 concentrations were measured using a Thermo Electron (Waltham, MA) ultraviolet photometric ozone analyzer Model 49i. Aliquots of NO were added to the reaction chamber from a 100 ppm tank (Butler Gas, McKees Rocks, PA) using a gas-tight syringe, and concentrations were measured using a Thermo Electron NOx analyzer Model 42i.

2.2. Impinger solvent comparison

Standard solutions of isopropyl nitrate, isobutyl nitrate, and 2-ethylhexyl nitrate were made in methanol. Aliquots of the standards were injected into collapsible chambers containing 80 L of air at 50% RH to give 100 ppb of each compound. Then, 40 L was pulled using a pump (URG 3000-02Q, Chapel Hill, NC) at 4 L/min, from the chamber through 10 mL of varying solvents (ethyl acetate, toluene, hexane, methanol, or water) in a 60 mL Teflon impinger (Savillex, Eden Prairie, MN). After collection, a 100 μL aliquot was taken from the impinger medium and placed in a 2 mL autosampler vial with a 100 μL glass insert (Restek, Bellefonte, PA). All samples were analyzed using an Agilent (Santa Clara, CA) 6890N GC with an Agilent μECD detector (Model: NER004P). Compound separation was achieved by an Agilent DB-5MS (0.25 mm I.D., 20 m long, 0.25 μm film thickness) column and the following GC oven parameters: 40 °C for 2 min, then 5 °C/min to 200 °C, then 25 °C/min to 280 °C and held for 5 min. One μL of each sample was injected in the splitless mode with the injector temperature at 130 °C. The μECD detector temperature was 300 °C and the N_2 makeup gas flow was 60 mL/min. Additional experiments were performed by varying the volume of solvent contained in the impinger as well as chilling the impinger before and during collection to prevent solvent evaporation.

2.3. Standard nitrate linear regression

The commercially available compounds isopropyl nitrate, isobutyl nitrate, and 2-ethylhexyl nitrate were used to determine the recovery efficiencies of the previously described system. The standards were injected into the 80 L chamber through the heated syringe injection port to give known final concentrations of 0.1, 0.5, and 1 ppb. Then, 40 L (1/2 total chamber volume) of the 50% RH chamber air was pulled through 10 mL of ethyl acetate and analyzed using GC-ECD as described above. In order to determine the efficiency of collection, each experiment was repeated where the nitrates were not injected into the chamber, but instead were injected directly into the ethyl acetate impinger after the 40 L had been drawn through. To demonstrate a 100% recovery efficiency, half of the volumes of the standard organic nitrate solution previously injected into the chamber were added to the impinger and analyzed by GC-ECD as described above. A linear regression was performed on the experimental data obtained from the measurement of the peak area of the compounds of known concentrations in the chamber.

2.4. Organic nitrate formation from terpene ozonolysis

In an 80 L volume of air at 50% RH, O_3 (20−100 ppb; 0.5−2.5 × 10^{12} molecules cm^{-3}) was added to 1.7 ppm (+)-α-pinene (4.3 × 10^{13} molecules cm^{-3}), nitric oxide (18−141 ppb; 0.5−3.5 × 10^{12} molecules cm^{-3}), and 283 ppm of cyclohexane, 232 ppm of hexane, or 265 ppm of pentane (7.0 × 10^{15}, 5.7 × 10^{15},

or 6.5×10^{15} molecules cm^{-3} respectively). The mixtures were allowed to react for 30 min. After the reaction, 40 L of the sample was collected, at 4 L/min, through 10 mL of ethyl acetate using an impinger (as described above). A table containing the alkyl nitrates formed and their retention times is provided in the Supplementary Information.

Alkyl nitrate reaction products were confirmed by synthesizing the compounds through two alternative methods: 1) photolyzing methyl nitrite to produce OH radicals to abstract hydrogen from cyclohexane to form the peroxyl or alkoxyl radical (Reactions (1) and (2b)/(3)) (Atkinson et al., 1981) and 2) reaction of the corresponding alkyl bromide with AgNO$_3$ (Ferris et al., 1953). Cyclohexyl nitrate synthesized from cyclohexyl bromide was purified by multiple extractions into methylene chloride as described by Ferris et al. (1953), and then the solvent was removed by vacuum evaporation.

3. Results and discussion

3.1. Impinger solvent comparison

Three commercially available organic nitrates (isopropyl nitrate, isobutyl nitrate, and 2-ethylhexyl nitrate) were used to determine the most suitable impinger solvent for capturing gas-phase organic nitrates. Fig. 1 shows the peaks obtained for the 2-ethylhexyl nitrate standard added to 80 L of 50% RH air and pulled through each of the solvents in an impinger. When comparing the solvents in an impinger, the rate of evaporation will affect the resulting signal intensity by increasing the concentration of solute through removal of solvent; therefore, the signal was normalized to the volumes of solvent recovered from the impinger. Ethyl acetate gave rise to the strongest signal for each of the organic nitrate standards and thus was chosen as the impinger medium for the remainder of the experiments in this study.

3.2. Standard nitrate linear regression

To determine the recovery efficiency of organic nitrates using the Teflon chamber and ethyl acetate impinger, known concentrations (0.1, 0.5, and 1 ppb) of the standards were added to the chamber. Air from the chamber was drawn through an ethyl acetate impinger at 4 L/min and an aliquot was analyzed using GC-ECD (Fig. 2). A second set of experiments was performed where the chamber contained no nitrates, but the nitrates were subsequently added to the ethyl acetate impinger after the 40 L had been drawn
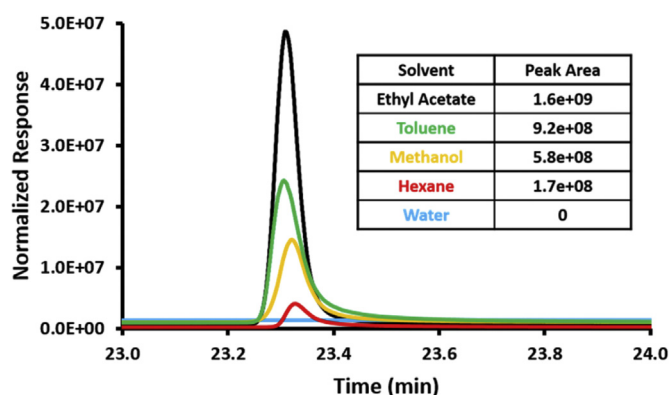

Fig. 2. Peak area versus concentration for isopropyl (A), isobutyl (B), and 2-ethylhexyl (C) nitrates added to ethyl acetate (spike) or injected into Teflon chambers then recovered by pulling through ethyl acetate impingers (chamber). Error bars represent the standard deviation of triplicate experiments.

through ("spike" data in Fig. 2). Although there were no nitrate species in the chamber for the spiked samples, it was important to pull the same volume of air through the ethyl acetate impingers as approximately 70% of the solvent is lost due to evaporation. The slopes of the chamber samples' trendlines shown in Fig. 2 were compared to the slopes of the corresponding spiked sample trendline to calculate a collection efficiency using Equation (4). Recovery efficiencies were 52.6, 53.1, and 63.3% for isopropyl, isobutyl, and 2-ethylhexyl nitrate respectively.

$$\text{Recovery efficiency } (\%) = (m_{chamber}/m_{spiked}) \times 100 \qquad (4)$$

The source of the loss of the remaining 35–50% is unknown. While some loss could be due to sparging in the impinger, when a second impinger was used in series, no breakthrough of the organic nitrate species were observed. Another possible source is wall loss. It has previously been reported that minimal alkyl nitrate wall loss is observed for compounds with fewer than eight carbons (Yeh and Ziemann, 2014); however, the chamber used in these experiments was 80 L compared to the 8200 L chamber used by Yeh and Ziemann. The smaller chamber used here has a higher surface-to-volume ratio than the Ziemann chamber, and therefore a higher amount of wall loss is likely.

Solvent	Peak Area
Ethyl Acetate	1.6e+09
Toluene	9.2e+08
Methanol	5.8e+08
Hexane	1.7e+08
Water	0

Fig. 1. Normalized GC-ECD chromatogram and peak areas of 2-ethylhexyl nitrate when captured using varying solvents. The peaks were normalized to the percent of solvent that evaporated during sampling to negate signal due to concentration of the solute.
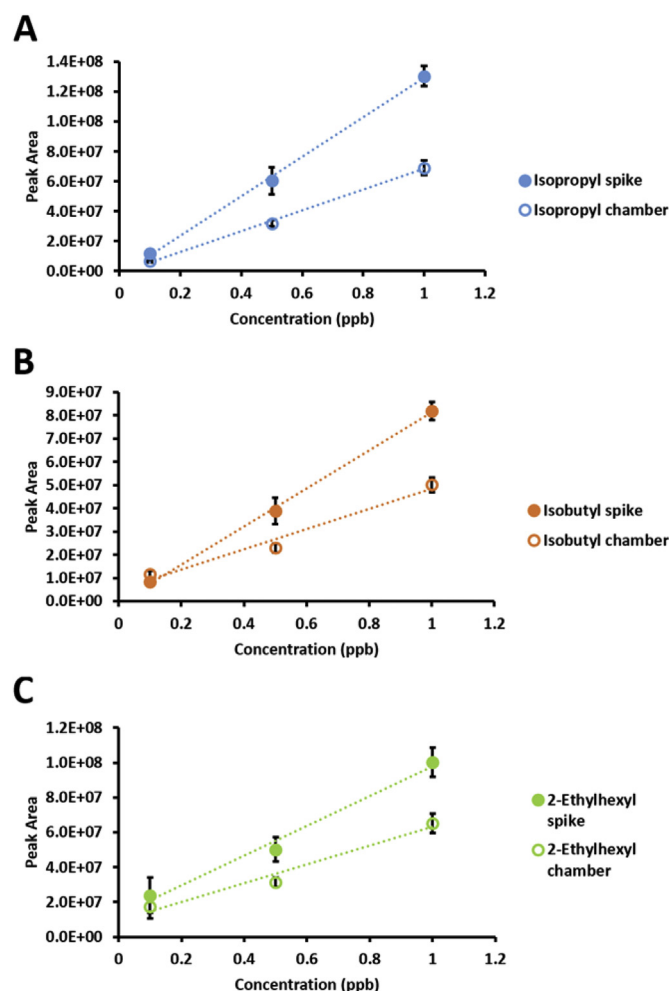
3.3. Organic nitrate formation from terpene ozonolysis

The chemistry of terpenes' reactions with ozone have been extensively studied and many reaction products have been identified (Hakola et al., 1994; Jackson et al., 2017; Jang and Kamens, 1999; Tillmann et al., 2010). However, terpene oxidation in the presence of NO has received less attention, and organic nitrate products, while hypothesized, have yet to be characterized (Aschmann et al., 2002; Nozière et al., 1999). This is likely due to the yields of individual nitrate products being below the limit of detection for many techniques. The Master Chemical Mechanism (v3.3.1) proposes more than 50 unique nitrate-containing products from α-pinene alone (Jenkin et al., 1997; Saunders et al., 2003). When ozone reacts with α-pinene, many multifunctional species are produced, including alcohols, carbonyls, and carboxylic acids. Hydroxyl radicals are also generated, with experimentally observed yields of 70–90% (Fig. 3) (Berndt et al., 2003). The hydroxyl radicals then have many reaction possibilities through hydrogen abstraction or addition to an unsaturated bond with an oxidation product, a different terpene molecule, or another compound altogether. All of these potential reaction pathways make the quantification of total organic nitrates difficult at low oxidant concentrations.

To optimize the conditions for detection of an organic nitrate species, cyclohexane was chosen as a hydroxyl radical scavenger due to its twelve equivalent hydrogens. When the hydroxyl radical abstracts a hydrogen from cyclohexane, the resulting single alkyl radical reacts with available oxygen to from a peroxyl radical (Fig. 3). The peroxyl radical can then react with NO to form an organic nitrate or an alkoxyl radical and NO_2. Since all 6 cyclohexane carbons are equivalent with respect to hydrogen abstraction, only one unique monofunctional nitrate is formed. Also, cyclohexane was present in excess of α-pinene to ensure the majority of •OH produced reacted with the alkane. The OH rate constants for cyclohexane and α-pinene are 7.49×10^{-12} (Atkinson and Aschmann, 1989) and 53.7×10^{-12} (Hakola et al., 1994), respectively. While the •OH rate constant is approximately $7\times$ faster for α-pinene, with a >100-fold excess of cyclohexane in the chamber, >95% of the OH generated should react with a cyclohexane molecule.

The peak for cyclohexyl nitrate was observed at 20.65 min. The identity of this peak was confirmed by two alternative methods of synthesizing cyclohexyl nitrate: reacting bromocyclohexane with $AgNO_3$ as well as initiating abstracting a hydrogen from cyclohexane by photolyzing methyl nitrite to generate OH radicals in the presence of NO. Both of these processes resulted in overlapping peaks at 20.65 min with experimental data supporting cyclohexyl nitrate as the identity of the product (Supplementary Fig. 1). Fig. 4 shows a series of control experiments, demonstrating that in order for the cyclohexyl nitrate peak at 20.65 min to be observed, all four components must be present in the reaction chamber.
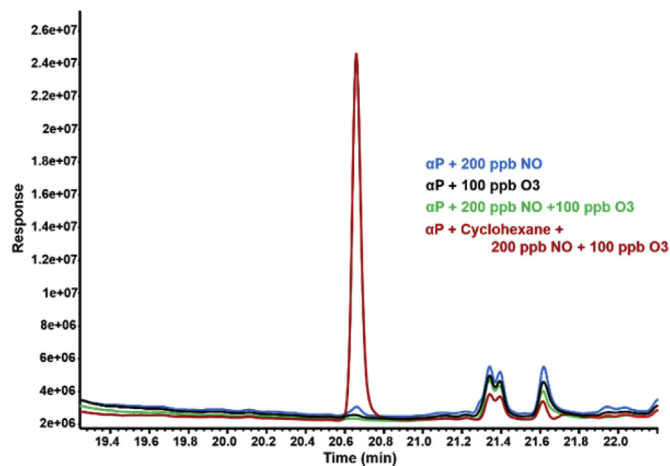
Fig. 4. GC-ECD chromatogram for the production of cyclohexyl nitrate when ozone is added to the chamber containing α-pinene, cyclohexane, and NO (red). Controls (blue, black, green) confirm that all species are involved in the formation mechanism. (For interpretation of the references to colour in this figure legend, the reader is referred to the web version of this article.)

3.4. Ozone and nitric oxide dependence

The detailed chemistry of organic nitrates has been extensively reviewed (Perring et al., 2013). There it is outlined how the relative importance of three possible chain termination reactions (formation of peroxides, formation of alkyl nitrates, and formation of HNO_3) change as a function of $[NO_x]$. For a given set of conditions, there is an intermediate NO_x concentration where $RONO_2$ production is maximized, while formation of peroxides and formation of HNO_3 are favored at lower and higher NO_x concentrations, respectively. By varying the concentrations of NO and O_3 introduced into the chamber, and plotting versus the peak area of cyclohexyl nitrate generated, this effect is visualized in Fig. 5.

Again the experimental conditions were optimized for the detection of a single product, cyclohexyl nitrate, which produced a higher ECD signal than if there were multiple organic nitrate species being formed, resulting in peaks below the instrument's detection limit. Furthermore, while "real-world" indoor environments are quite complicated with many potential reaction sites for hydroxyl radicals or NO, by keeping the chamber conditions simplified, the upper limit of organic nitrate formation for a given set of oxidant conditions can be measured. By generating a calibration curve using the synthesized cyclohexyl nitrate standard, we are able to calculate yields of cyclohexyl nitrate using the equation

$$x = (y-b)/(m \times \text{Recovery efficiency}) \tag{5}$$

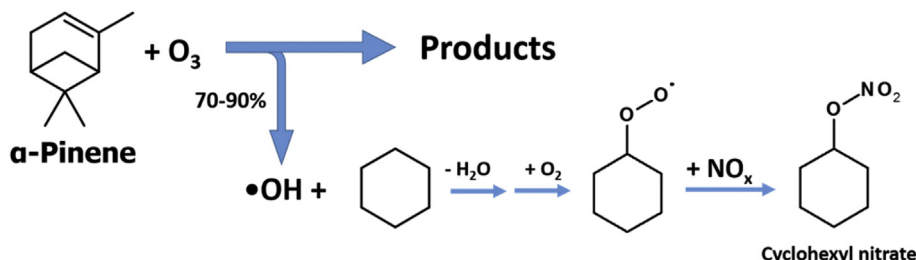where x is concentration of cyclohexyl nitrate, y is the integrated

Fig. 3. Reaction scheme showing the formation of cyclohexyl nitrate initiated by α-pinene ozonolysis.
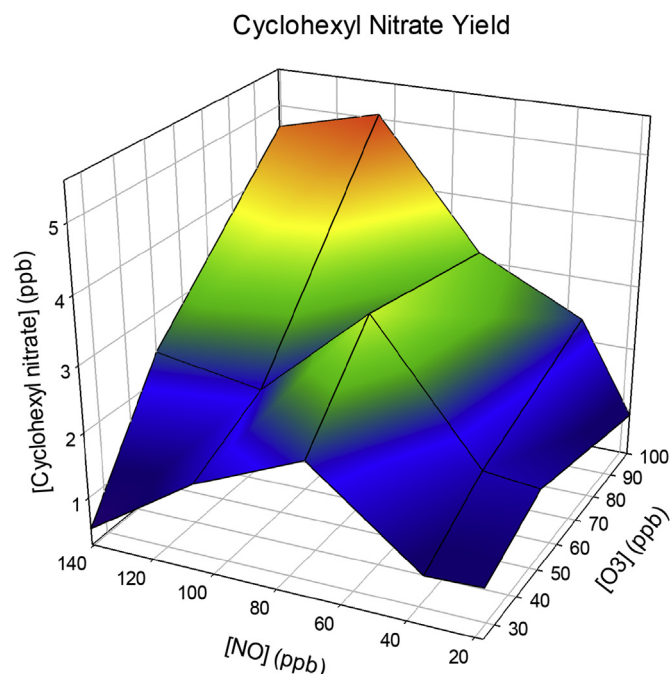
Cyclohexyl Nitrate Yield

Fig. 5. Plot of cyclohexyl nitrate peak area versus [NO] and [O₃] added to the chamber. Each vertex is the mean of triplicate experiments. Yield was determined by generating a calibration curve for synthesized cyclohexyl nitrate.

peak area, b is the y-intercept, and m is the slope of the calibration curve (Supplementary Fig. 2). The recovery efficiency was estimated to be 60% based on the values calculated for the nitrate standards. As seen in Fig. 5, the maximum concentration of cyclohexyl nitrate generated was 5 ppb, suggesting that up to 5 ppb of organic nitrates may be formed in an environment with 100 ppb O₃ and 105 ppb NO.

When these experiments were reproduced with different alkanes acting as scavengers, such as pentane or hexane (Fig. 6A&B), the overall alkyl nitrate yield trend was conserved. This demonstrates that in the presence of excess alkanes, organic nitrate yield may be maximized at a similar O₃/NO concentration regardless of the nature of the alkane. Small differences in yields are likely; however, as Yeh and Ziemann calculated alkyl nitrate yields slightly increase as carbon number increases (0.210 for C_7 to 0.294 for C_{16}) (Yeh and Ziemann, 2014). It is worth noting that as opposed to cyclohexane which has only one unique hydrogen for abstraction, pentane and hexane each have 3 unique hydrogens and for the generation of the plots in Fig. 6, the sum of the areas of the three nitrate peaks were used. The ratio of the peaks themselves was constant (8:8:1 for hexane and 6:9:1 for pentane), suggesting that a secondary carbon radical is 8–11 times more favorable than a primary carbon radical. This is more than the theoretical calculation using EPA's Estimation Programs Interface Suite of 6.9–8.5 times more favorable (EPA, 2017), but slightly less than those reported elsewhere (Arey et al., 1990; Yeh and Ziemann, 2014).

A limitation of this study is the static nature of the experiments. Indoor air is a dynamic system, where air and its contaminants are constantly being exchanged between the inside and outside environments. Both NO and O₃ can be transported indoors from the outside, but they will not be present at high concentrations at the same time as O₃ will rapidly react with NO to form NO₂. Weschler, Shields, and Naik demonstrated this by measuring indoor concentrations of O₃, NO, and NO₂ over 14 months at a location in southern California (Weschler et al., 1994). Indoor concentrations of O₃ and NO reached above 55 and 250 ppb, respectively, but only one species was present at a time (NO at night/mornings & O₃ in the afternoon/evenings). Therefore the experiments described here more closely mimic a scenario where O₃ is transported indoors to an environment with an NO-emitting source, such as a cooking appliance or an unvented heater.

While gas-phase organic nitrates were the focus of this study, Carslaw et al. predicted that organic nitrates play an even greater role in secondary organic aerosol (SOA) than in the gas-phase precursors (Carslaw et al., 2012). A model that followed limonene oxidation pathways in detail during simulated cleaning activities predicted that carbonyls and peroxyacetyl nitrates are the most common gas-phase species formed; however, in aerosols, peroxides, carbonyls, and organic nitrates dominate. Future studies will investigate nitrated species in the aerosol fraction as well as gas-phase while taking into consideration air exchange effects. The addition of nitrogen dioxide into the system will also be investigated with the goal of elucidating the influence of the different
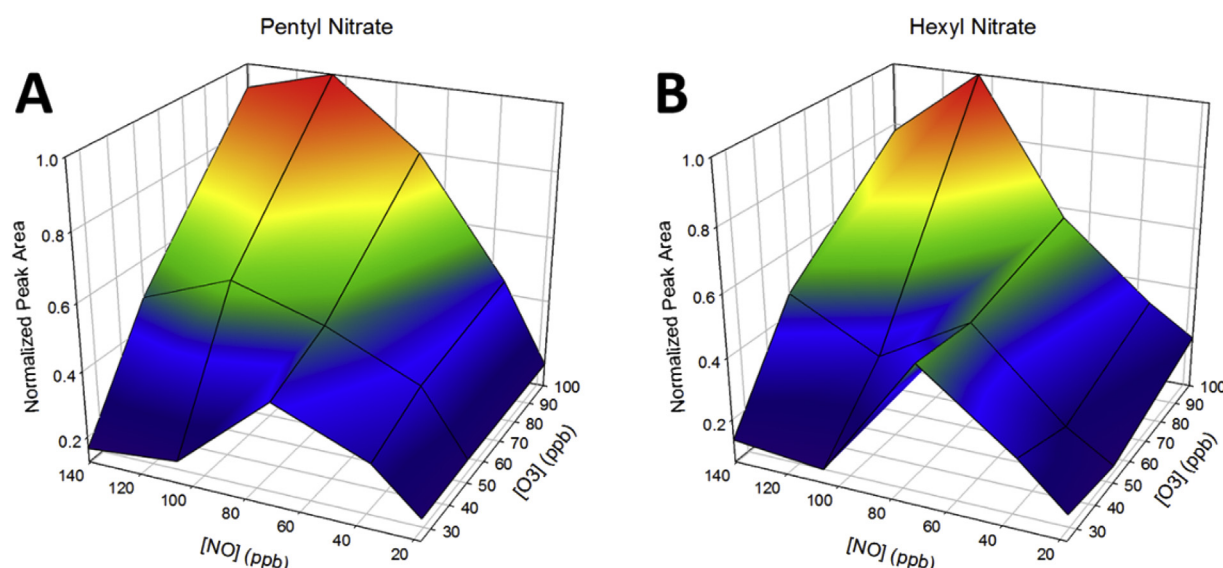
Pentyl Nitrate

Hexyl Nitrate

Fig. 6. Plot of summed (A) pentyl nitrate peak areas and (B) hexyl nitrate peak areas versus [NO] and [O₃] added to the chamber. Each vertex is the mean of triplicate experiments.

formation pathways on total alkyl nitrate yield.

4. Conclusion

In this study, alkyl nitrates were formed from the reaction of ozone and α-pinene in the presence of an alkane and NO. Up to 5 ppb organic nitrate formation was observed when 100 ppb O_3 was introduced to a chamber containing 105 ppb NO and excess α-pinene and cyclohexane. These experiments demonstrate that alkyl nitrates may be formed with conditions found in indoor environments. Organic nitrates are often complex multifunctional species that remain difficult to observe by chromatography at ambient abundances; however, these simplified GC-ECD studies have confirmed the identity of a series of $RONO_2$ compounds formed during chamber studies. These measurements are consistent with observations and predictions of alkyl nitrate formation in the atmosphere. Further studies on both the formation of alkyl nitrates indoors and the epidemiological effect of these compounds are needed to fully characterize the exposures that occur in the indoor environment.

Disclaimer

The findings and conclusions in this report are those of the authors and do not necessarily represent the views of the National Institute for Occupational Safety and Health.

Appendix A. Supplementary data

Supplementary data related to this article can be found at https://doi.org/10.1016/j.atmosenv.2017.10.002.

References

Arey, J., Atkinson, R., Aschmann, S.M., 1990. Product study of the gas-phase reactions of monoterpenes with the OH radical in the presence of NO x. J. Geophys. Res. Atmos. 95, 18539—18546.

Aschmann, S.M., Atkinson, R., Arey, J., 2002. Products of reaction of OH radicals with α-pinene. J. Geophys. Res. Atmos. 107, 6—7. ACH 6-1-ACH.

Atkinson, R., Arey, J., 2003. Atmospheric degradation of volatile organic compounds. Chem. Rev. 103, 4605—4638.

Atkinson, R., Aschmann, S.M., 1989. Rate constants for the gas-phase reactions of the OH radical with a series of aromatic hydrocarbons at 296 ± 2 K. Int. J. Chem. Kinet. 21, 355—365.

Atkinson, R., Carter, W.P.L., Winer, A.M., 1983. Effects of temperature and pressure on alkyl nitrate yields in the nitrogen oxide (NOx) photooxidations of n-pentane and n-heptane. J. Phys. Chem. 87, 2012—2018.

Atkinson, R., Carter, W.P.L., Winer, A.M., Pitts, J.N., 1981. An experimental protocol for the determination of OH radical rate constants with organics using methyl nitrite photolysis as an OH radical source. J. Air Pollut. Control Assoc. 31, 1090—1092.

Bello, A., Quinn, M.M., Perry, M.J., Milton, D.K., 2009. Characterization of occupational exposures to cleaning products used for common cleaning tasks-a pilot study of hospital cleaners. Environ. Health 8, 11—11.

Berndt, T., Böge, O., Stratmann, F., 2003. Gas-phase ozonolysis of α-pinene: gaseous products and particle formation. Atmos. Environ. 37, 3933—3945.

Carslaw, N., Mota, T., Jenkin, M.E., Barley, M.H., McFiggans, G., 2012. A significant role for nitrate and peroxide groups on indoor secondary organic aerosol.

Environ. Sci. Technol. 46, 9290—9298.

Day, D.A., Farmer, D.K., Goldstein, A.H., Wooldridge, P.J., Minejima, C., Cohen, R.C., 2009. Observations of NO_x, ΣPNs, ΣANs, and HNO_3 at a rural site in the California Sierra Nevada mountains: summertime diurnal cycles. Atmos. Chem. Phys. 9, 4879—4896.

EPA, U., 2017. In: Agency, U.S.E.P. (Ed.), Estimation Programs Interface Suite for Microsoft Windows, 4.11 ed. Washington, DC, USA.

Ferris, A.F., McLean, K.W., Marks, I.G., Emmons, W.D., 1953. Metathetical reactions of silver salts in solution. III. The synthesis of nitrate Esters1. J. Am. Chem. Soc. 75, 4078—4078.

Forester, C.D., Wells, J.R., 2011. Hydroxyl radical yields from reactions of terpene mixtures with ozone. Indoor Air 21, 400—409.

Gerster, F.M., Vernez, D., Wild, P.P., Hopf, N.B., 2014. Hazardous substances in frequently used professional cleaning products. Int. J. Occup. Environ. Health 20, 46—60.

Hakola, H., Arey, J., Aschmann, S.M., Atkinson, R., 1994. Product formation from the gas-phase reactions of OH radicals and O3 with a series of monoterpenes. J. Atmos. Chem. 18, 75—102.

Ham, J.E., Harrison, J.C., Jackson, S.R., Wells, J.R., 2016. Limonene ozonolysis in the presence of nitric oxide: gas-phase reaction products and yields. Atmos. Environ. 132, 300—308.

Ham, J.E., Jackson, S.R., Harrison, J.C., Wells, J.R., 2015. Gas-phase reaction products and yields of terpinolene with ozone and nitric oxide using a new derivatization agent. Atmos. Environ. 122, 513—520.

Jackson, S.R., Ham, J.E., Harrison, J.C., Wells, J.R., 2017. Identification and quantification of carbonyl-containing α-pinene ozonolysis products using O-tert-butylhydroxylamine hydrochloride. J. Atmos. Chem. 74, 325.

Jang, M., Kamens, R.M., 1999. Newly characterized products and composition of secondary aerosols from the reaction of α-pinene with ozone. Atmos. Environ. 33, 459—474.

Jenkin, M.E., Saunders, S.M., Pilling, M.J., 1997. The tropospheric degradation of volatile organic compounds: a protocol for mechanism development. Atmos. Environ. 31, 81—104.

Monks, P.S., 2005. Gas-phase radical chemistry in the troposphere. Chem. Soc. Rev. 34, 376—395.

Nazaroff, W.W., Weschler, C.J., 2004. Cleaning products and air fresheners: exposure to primary and secondary air pollutants. Atmos. Environ. 38, 2841—2865.

Nozière, B., Barnes, I., Becker, K.-H., 1999. Product study and mechanisms of the reactions of α-pinene and of pinonaldehyde with OH radicals. J. Geophys. Res. Atmos. 104, 23645—23656.

Perring, A.E., Pusede, S.E., Cohen, R.C., 2013. An observational perspective on the atmospheric impacts of alkyl and multifunctional nitrates on ozone and secondary organic aerosol. Chem. Rev. 113, 5848—5870.

Rollins, A.W., Smith, J.D., Wilson, K.R., Cohen, R.C., 2010. Real time in situ detection of organic nitrates in atmospheric aerosols. Environ. Sci. Technol. 44, 5540—5545.

Saunders, S.M., Jenkin, M.E., Derwent, R.G., Pilling, M.J., 2003. Protocol for the development of the Master Chemical Mechanism, MCM v3 (Part A): tropospheric degradation of non-aromatic volatile organic compounds. Atmos. Chem. Phys. 3, 161—180.

Tillmann, R., Hallquist, M., Jonsson, Å.M., Kiendler-Scharr, A., Saathoff, H., Iinuma, Y., Mentel, T.F., 2010. Influence of relative humidity and temperature on the production of pinonaldehyde and OH radicals from the ozonolysis of α-pinene. Atmos. Chem. Phys. 10, 7057—7072.

Weschler, C.J., Shields, H.C., 1996. Production of the hydroxyl radical in indoor air. Environ. Sci. Technol. 30, 3250—3258.

Weschler, C.J., Shields, H.C., 1997. Potential reactions among indoor pollutants. Atmos. Environ. 31, 3487—3495.

Weschler, C.J., Shields, H.C., Naik, D.V., 1994. Indoor chemistry involving O3, NO, and NO2 as evidenced by 14 Months of measurements at a site in southern California. Environ. Sci. Technol. 28, 2120—2132.

Wolkoff, P., Schneider, T., Kildesø, J., Degerth, R., Jaroszewski, M., Schunk, H., 1998. Risk in cleaning: chemical and physical exposure. Sci. Total Environ. 215, 135—156.

Yeh, G.K., Ziemann, P.J., 2014. Alkyl nitrate formation from the reactions of C8—C14 n-alkanes with OH radicals in the presence of NOx: measured yields with essential corrections for gas—wall partitioning. J. Phys. Chem. A 118, 8147—8157.